

# 3D printing for sizing left atrial appendage closure device: head-to-head comparison with computed tomography and transoesophageal echocardiography



Michaela M. Hell<sup>1\*</sup>, MD; Stephan Achenbach<sup>1</sup>, MD; In Seong Yoo<sup>2</sup>, Dipl.-Ing; Joerg Franke<sup>2</sup>, Dr.-Ing; Florian Blachutzik<sup>1</sup>, MD; Jens Roether<sup>1</sup>, MD; Verena Graf<sup>1</sup>, MD; Dorette Raaz-Schrauder<sup>1</sup>, MD; Mohamed Marwan<sup>1</sup>, MD; Christian Schlundt<sup>1</sup>, MD

1. Department of Cardiology, Faculty of Medicine, Friedrich-Alexander-University Erlangen-Nürnberg, Erlangen, Germany; 2. Institute for Factory Automation and Production Systems, Friedrich-Alexander-University Erlangen-Nürnberg, Erlangen, Germany

## KEYWORDS

- innovation
- left atrial appendage (LAA) closure
- multislice computed tomography (MSCT)

## Abstract

**Aims:** Device sizing for LAA closure using transoesophageal echocardiography (TEE) can be challenging due to complex LAA anatomy. We investigated whether the use of 3D-printed left atrial appendage (LAA) models based on preprocedural computed tomography (CT) permits accurate device sizing.

**Methods and results:** Twenty-two (22) patients (73±8 years, 55% male) with atrial fibrillation requiring anticoagulation at high bleeding risk underwent LAA closure (WATCHMAN device). Preprocedurally, LAA was sized by TEE and third-generation dual-source CT. Based on CT, 3D printing models of LAA anatomy were created for simulation of device implantation. Device compression was assessed in a CT scan of the 3D model with the implanted device. Implantation was successful in all patients. Mean LAA ostium diameter based on TEE was 22±4 mm and based on CT 25±3 mm (p=0.014). Predicted device size based on simulated implantation in the 3D model was equal to the device finally implanted in 21/22 patients (95%). TEE would have undersized the device in 10/22 patients (45%). Device compression determined in the 3D-CT model corresponded closely with compression upon implantation (16±3% vs. 18±5%, r=0.622, p=0.003).

**Conclusions:** Patient-specific CT-based 3D printing models may assist device selection and prediction of device compression in the context of interventional LAA closure.

\*Corresponding author: Department of Cardiology, Faculty of Medicine, Friedrich-Alexander-University Erlangen-Nürnberg, Ulmenweg 18, 91054 Erlangen, Germany. E-mail: michaela.hell@uk-erlangen.de

## Abbreviations

<b>CT</b>	computed tomography
<b>LAA</b>	left atrial appendage
<b>TEE</b>	transoesophageal echocardiography
<b>3D</b>	three-dimensional

## Introduction

The relationship between atrial fibrillation and ischaemic events has been established<sup>1</sup>. Traditionally, oral anticoagulation is the therapy of choice to prevent thromboembolic complications<sup>2</sup>. Occlusion of the left atrial appendage (LAA) provides effective stroke prevention and is clinically used in patients with high bleeding risk on anticoagulation therapy<sup>1</sup>. For the WATCHMAN™ device (Boston Scientific, Marlborough, MA, USA), non-inferiority regarding safety and efficiency compared to warfarin has been demonstrated in randomised trials<sup>3,4</sup>.

Correct sizing is crucial for successful and safe device implantation. Serious complications are reported in 4% of cases<sup>4</sup>. Intraprocedurally, imaging by angiography and transoesophageal echocardiography (TEE) is used to confirm complete sealing of the LAA by the occluder, exact device positioning and appropriate compression of the occluder prior to device release. A compression of 8-20% of the original occluder size is desirable to prevent device embolisation<sup>5</sup>. Due to the complex three-dimensional (3D) and highly variable LAA anatomy, imaging is difficult, and currently used imaging modalities have limited value to predict the appropriate device size. Intraprocedural device removal and re-implantation of a differently sized model therefore frequently become necessary.

3D printing has emerged as a tool for planning structural heart interventions<sup>6-8</sup>. In this prospective study, we systematically compared computed tomography (CT)-based 3D model prediction of device size and compression to the established TEE-based approach. Preprocedurally, an occluder was implanted in the 3D model based on CT sizing and visually assessed regarding positioning, anchoring and sealing. Furthermore, compression was quantified in a CT scan of the model with an implanted occluder.

## Methods

### PATIENTS

Twenty-nine consecutive patients with atrial fibrillation and at high risk for stroke (CHA<sub>2</sub>DS<sub>2</sub>-VASc score  $\geq 2$ ) and bleeding (HAS-BLED score  $\geq 3$  or history of major bleeding complications on anticoagulant therapy) undergoing LAA occlusion with the WATCHMAN device were screened for enrolment between October 2015 and January 2017. Three patients showed an impaired renal function (GFR  $< 30$  ml/min/1.73 m<sup>2</sup>), and one patient refused informed consent. Two patients demonstrated an LAA thrombus, and one patient had LAA dimensions exceeding available occluder sizes. Finally, 22 patients participated in the study (Figure 1). The local institutional review board approved the study.

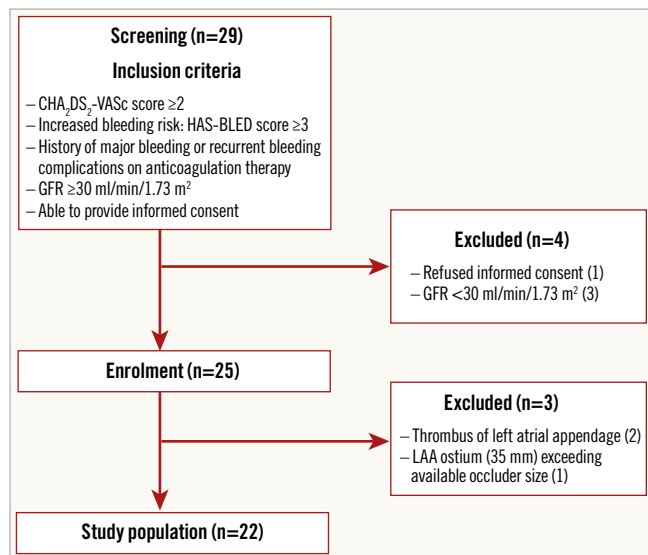


**Figure 1.** Study flow chart. Out of 29 patients initially screened for participation in the study, 22 patients were finally included in the cohort.

### TRANSOESOPHAGEAL ECHOCARDIOGRAPHY ASSESSMENT

All patients underwent preprocedural TEE for assessing LAA orifice diameter and length at 0°, 45°, 90° and 135° by an operator with clinical experience regarding TEE in the context of LAA occlusion (more than 100 cases) and blinded to CT and 3D model sizing results. Patients were pre-hydrated with 1,000 ml intravenous balanced electrolyte solution to ensure sufficient LAA filling. Device selection by TEE was based on maximum ostial diameters according to the manufacturer's instructions.

### CT IMAGE ACQUISITION

For comparable LAA filling conditions, CT imaging was performed immediately after TEE using third-generation dual-source CT (SOMATOM® Force; Siemens Healthineers, Forchheim, Germany) and a prospectively ECG-triggered high-pitch spiral acquisition mode<sup>9</sup>. Tube output was adjusted to patient's BMI (80-100 kV, 450-650 mAs); acquisition was performed at 70% of the R-peak-to-R-peak interval. Patients with a heart rate  $> 60$  beats/min received beta-blockers. Contrast transit time was assessed by the test bolus technique. For angiography, 60 mL of contrast agent (350 mg iodine/mL, Iomeron®; Bracco Imaging, Milan, Italy) was injected via an antecubital vein followed by a 60 mL flush (80% saline, 20% contrast agent) at 6 mL/s.

### CT-BASED MEASUREMENT OF LAA DIMENSIONS

Analyses were performed on an off-line workstation (Multimodality Workplace; Siemens Healthcare, Erlangen, Germany) by an operator experienced in CT imaging and analysis in the context of LAA occlusion (more than 100 cases) and blinded to TEE results. LAA ostium diameters, length, morphology (chicken wing, windsock, cauliflower or cactus) and number of lobes were assessed in two-dimensional (2D) oblique transverse views with the three planes

locked at a 90° angle<sup>10,11</sup>. CT-based device selection was carried out using the same manufacturer specifications as used for TEE sizing.

### CREATION OF 3D MODELS

For creating an individual 3D model based on CT data, the LAA, the left superior pulmonary vein proximal segment and the adjacent part of the left atrium were manually segmented slice by slice on a multimodality workstation. DICOM data were imported in the 3D-slicer open-source software platform and converted into 3D-printable standard tessellation language to print a 3D relief (Ultimaker 2; Ultimaker B.V., Geldermalsen, the Netherlands). Next, a negative model was created using a two-component silicone rubber vulcanising at room temperature (ELASTOSIL P7670 A/B; Wacker Chemie AG, Munich, Germany) (**Figure 2**). Generation of the 3D print and corresponding model requires approximately five to six hours in total; the pure material cost is approximately 20 euros.

### SIMULATION OF LAA DEVICE IMPLANTATION

Based on CT sizing and blinded to TEE results, an occluder was inserted into the 3D model by the interventional cardiologist performing the later occluder implantation with an experience of more than 125 LAA occlusion procedures. Complete engagement of all anchors and sealing of the LAA ostium was visually assessed; a stability test (tug test) was performed. For prediction of device compression, CT images of the 3D model with the implanted device were acquired (70 kV, 450 mAs) in high-pitch spiral acquisition and reconstructed with a medium sharp convolution kernel (“B40”), a 0.6 mm slice thickness and a 0.4 mm increment. Two maximum intensity projections (10 mm thickness), one carefully aligned with the longitudinal axis of the implanted occluder and one aligned with the LAA ostium, were used to visualise the device<sup>12</sup>. The maximum device diameter was measured and compression (in %) was calculated as

$$\left(1 - \frac{\text{maximum diameter of implanted device}}{\text{original device diameter}}\right) \times 100.$$

The device size was rated as “optimal” if all anchors were completely engaged, the ostium was completely sealed, the tug test was positive and compression was within the optimal range (8-20%)<sup>5</sup>. If the device size based on CT measurements was inappropriate in the 3D model, the next larger and smaller device sizes were assessed until the optimal device size was found. Imaging cascade is shown in **Figure 3**.

### LAA PROCEDURE

The WATCHMAN device was implanted via a transfemoral transseptal approach using a catheter-based delivery system. All patients were pre-hydrated to achieve a left atrial pressure >12 mmHg. The implantation procedure was performed under fluoroscopic and TEE guidance<sup>13</sup>. Initial device size was chosen based on 3D model measurements; the interventional cardiologist was blinded to the preprocedural TEE and CT results. Only optimally implanted devices, defined as a completely sealed ostium, a positive tug test and a compression within optimal range, were accepted and, if necessary, partial or full recapture including a change in occluder size was performed. Compression was measured periprocedurally by TEE using the maximum diameter of the device. Post-procedurally, antiplatelet therapy consisted of 100 mg acetylsalicylic acid and 75 mg clopidogrel daily for six months.

### FOLLOW-UP

A clinical and TEE follow-up was performed in all patients after 30 days. Adverse events including severe bleeding, haemodynamically significant pericardial effusion, occluder embolisation, stroke, mortality, and all death were assessed. Presence of device-attached thrombus and peri-device leak were examined by TEE.

### STATISTICAL ANALYSIS

Statistical analysis was performed using SPSS software, Version 21 (IBM Corp., Armonk, NY, USA). Continuous variables were

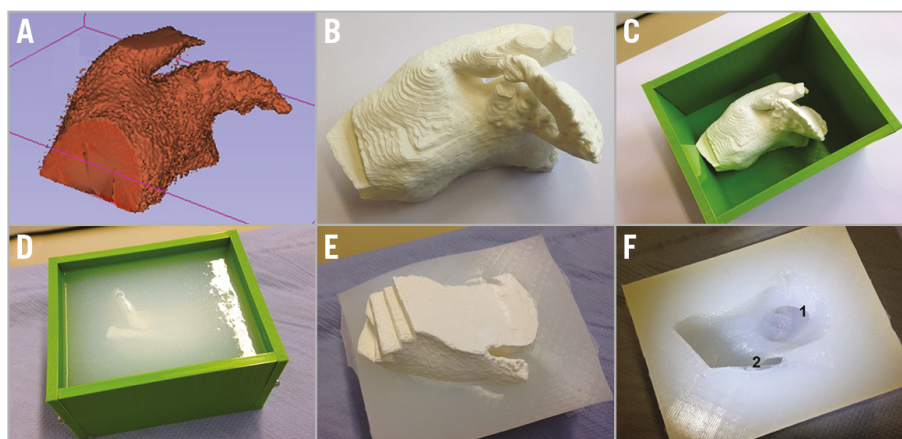


**Figure 2.** Generation of 3D model. From a standard tessellation language file (A), a 3D relief was printed (B). The 3D-printed positive model was fixed in a casting mould (C) and a negative model was created by filling the mould with two-component silicone rubber vulcanising at room temperature (D & E). After curing and demoulding, the plastic model was removed from the silicone rubber cast leaving the 3D structures (F) displaying the left atrial appendage (1) and the proximal left upper pulmonary vein (2).

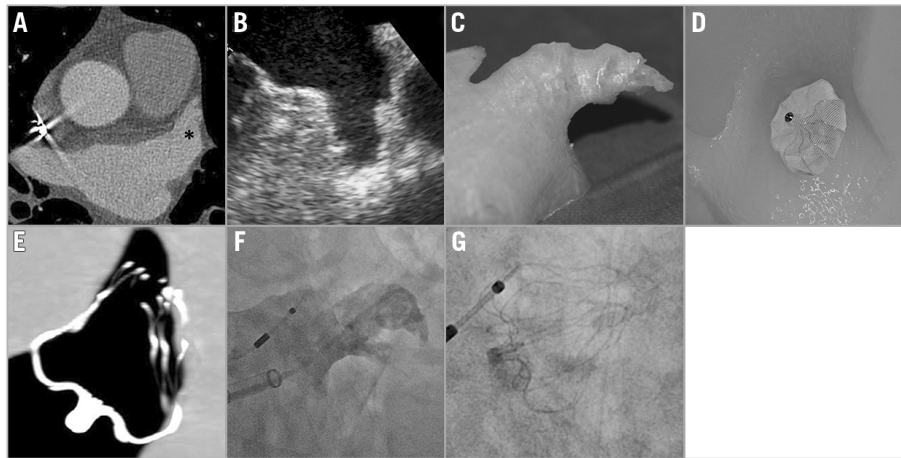


**Figure 3.** Left atrial appendage (LAA) imaging and device implantation in a 71-year-old male. A) CT angiography (\* LAA). B) Transoesophageal echocardiography. C) 3D print LAA model. D) 3D model with implanted device. E) CT scan of 3D model with implanted device. F) Fluoroscopy LAA imaging. G) Implanted device.

expressed as mean±SD, categorical variables as frequencies and percentage. A chi-squared test ( $\chi^2$  test) was used for comparison between categorical variables. Parametric data were compared using the t-test and non-parametric data using the Mann-Whitney U test for continuous variables. Association between compression of the implanted occluder and 3D model-predicted compression was assessed by Pearson correlation coefficient. All tests performed were two-sided and  $p < 0.05$  was considered to be statistically significant.

## Results

### BASELINE CHARACTERISTICS AND OUTCOME

Mean patient age was 73±8 years; 55% of the patients were male. The mean CHA<sub>2</sub>DS<sub>2</sub>-VASc score was 3±1, and the mean HAS-BLED score was 4±1. **Table 1** presents baseline characteristics. The periprocedural drug regimen is illustrated in **Table 2**. Intraprocedural pressure of the left atrium was >12 mmHg in all patients. LAA closure was successfully performed in all patients. Intraprocedural TEE revealed a complete device sealing of the LAA in all patients. During implantation, seven patients (32%) showed sinus rhythm, and 15 patients (68%) atrial fibrillation. There was no case of in-hospital death or death within the first 30 days (**Table 3**).

### PREPROCEDURAL ASSESSMENT OF MORPHOLOGY AND SIZING BY TEE, CT AND 3D-CT MODEL

CT-based assessment of LAA shape revealed “chicken wing” morphology in five patients (23%), “cactus” morphology in six patients (27%), “cauliflower” morphology in eight patients (36%) and “windsock” morphology in three patients (14%). Fourteen patients (64%) had an unilobular LAA and eight patients (36%) a bilobular LAA. CT-based measurements of ostium diameter (25±3 vs. 22±4 mm,  $p=0.014$ ) and depth (38±5 vs. 32±6 mm,  $p < 0.001$ ) were significantly larger than TEE-based measurements (**Table 4**). Device implantation according to CT-based LAA diameters into the 3D model revealed a correct size selection in 18 cases (81%). In the other four cases, the 3D model

recommended the next smaller device size for optimal fitting and compression (**Table 5**).

### AGREEMENT OF TEE AND 3D MODEL-BASED PREDICTION DEVICE SIZE WITH FINAL IMPLANTATION

3D model-based prediction of occluder size was in agreement with the finally implanted occluder in 21/22 cases (95%). In one case, the predicted size was too small, showing a slight leakage. The interventional cardiologist performed a full recapture with a device change to the next larger size. Angiographic and echocardiographic assessment revealed no leakage and a compression within optimal range. CT-based device size prediction was congruent with the final device size in 17 patients (77%), while four cases (18%) were oversized and one case (5%) undersized (**Figure 4**). TEE-based size suggestion was congruent with the finally implanted size in 12 cases (55%). For the other 10 cases, TEE-based device sizing was too small. Compression measured periprocedurally by TEE after implantation was within the optimal range (8-20%) in 17 patients (77%); five patients had a compression between 20% and 24%. Compression of implanted occluders corresponded well with the 3D-CT model-predicted compression (17.6±4.7 vs. 15.6±3.2%,  $r=0.622$ ,  $p=0.003$ ) (**Figure 5**).

### FOLLOW-UP

At 30-day TEE follow-up, 20 patients (90%) demonstrated complete LAA sealing by the occluder, while two patients had a minimal leakage ( $\leq 3$  mm). There was no serious adverse event. In one patient with polycythaemia vera and *a priori* unknown heparin-induced thrombocytopenia, a device-attached thrombus was found incidentally by TEE before electrocardioversion 19 days after implantation. This disappeared under phenprocoumon without any embolic event.

## Discussion

In this prospective study, we demonstrated that the manufacturing of LAA models using 3D printing based on CT data provides

**Table 1. Baseline characteristics.**

Variable	Total cohort n=22
<b>Clinical characteristics</b>	
Age (yrs)	73±8
Male sex, n (%)	12 (55)
Body mass index (kg/m <sup>2</sup> )	27±6
Cardiovascular risk factors, n (%)	
Hypertension	20 (91)
Hyperlipidaemia	9 (41)
Diabetes mellitus	3 (14)
Tobacco use	1 (5)
Family history of coronary artery disease	5 (23)
CHA <sub>2</sub> DS <sub>2</sub> -VASc score	
2, n (%)	5 (23)
3	7 (32)
4	7 (32)
5	1 (5)
6	2 (9)
HAS-BLED score	
3, n (%)	13 (59)
4	7 (32)
5	2 (9)
Atrial fibrillation, n (%)	
Paroxysmal	11 (50)
Persistent	2 (9)
Permanent	9 (41)
Congestive heart disease, n (%)	2 (9)
Vascular disease, n (%)	10 (46)
Abnormal renal function, n (%)	5 (23)
Abnormal liver function, n (%)	2 (10)
Prior ischaemic stroke, n (%)	1 (5)
Prior haemorrhagic stroke, n (%)	7 (32)
Prior major bleeding complications on anticoagulation therapy, n (%)	19 (86)
Ejection fraction, %	55±12
Ejection fraction <35%, n (%)	2 (9)
Left atrium size, mm	47±6

**Table 2. Periprocedural drug regimen.**

Anticoagulation	Pre-implant	Post-implant
None	2 (9)	0 (0)
Single APT	2 (9)	0 (0)
Dual APT	3 (14)	22 (100)
Vitamin-K dependent agents	10 (46)	0 (0)
Novel oral anticoagulants	7 (32)	0 (0)
Low molecular weight heparin	1 (5)	0 (0)

Values are n (%). Pre-implantation information exceeds n=22, as some patients received both APT and anticoagulation. APT: antiplatelet therapy

a feasible, non-invasive technique for visualisation of patient-specific LAA anatomy and allows preprocedural WATCHMAN device sizing, including simulation of occluder implantation with accurate prediction of device compression.

We found a 95% agreement rate for 3D model-based sizing compared to the finally implanted WATCHMAN occluder. The incidence of serious adverse events within 30 days was 4.5%, corresponding to results from multicentre registries including EWOLUTION, PROTECT AF and PREVAIL<sup>3,4,14</sup>. TEE-based

**Table 3. Procedural success and outcome.**

Variable	Total cohort n=22
Procedural success	22 (100)
Serious adverse events (SAE) within 30 days	1 (4.5)
Device/procedure-related SAE	0 (0)
Bleeding SAE	0 (0)
Thrombus on the device	1 (4.5)
All deaths	0 (0)
Haemodynamically relevant pericardial effusion	0 (0)
Stroke	0 (0)
Occluder embolisation	0 (0)
In-hospital mortality	0 (0)
30-day mortality	0 (0)

Values are n (%).

**Table 4. LAA dimensions and device sizing by TEE, CT and 3D model, and agreement with finally implanted occluder size.**

Variable		TEE-based	CT-based	p-value	
LAA dimensions, mm	Ostium	22±4	25±3	0.014	
	Depth	32±6	38±5	<0.001	
		TEE-based	CT-based	3D model	Implantation
Sizing, n (%)	21 mm	8 (36)	2 (8)	3 (14)	3 (14)
	24 mm	6 (27)	3 (14)	3 (14)	3 (14)
	27 mm	3 (14)	7 (32)	7 (32)	7 (32)
	30 mm	5 (23)	7 (32)	7 (32)	6 (26)
	33 mm	0 (0)	3 (14)	2 (8)	3 (14)
Agreement with finally implanted occluder size, n (%)		12 (55)	17 (77)	21 (95)	

CT: computed tomography; LAA: left atrial appendage; TEE: transoesophageal echocardiography

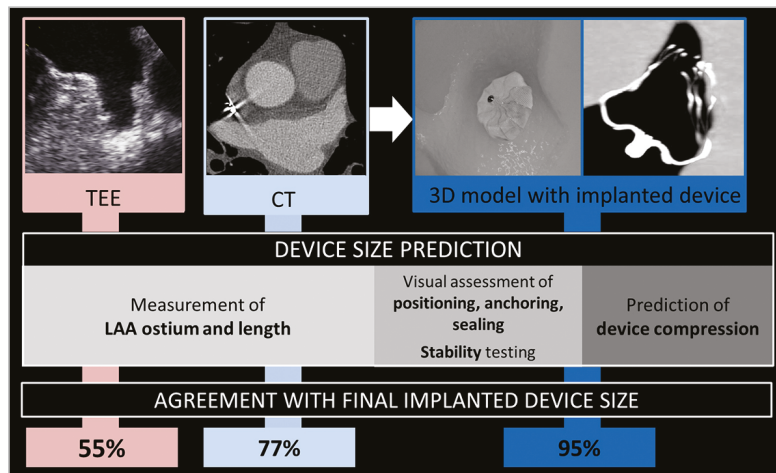


**Figure 4.** Device size prediction by transoesophageal echocardiography (TEE), computed tomography (CT) and 3D model with implanted device and agreement with final implanted device size.

sizing has previously been shown to have the lowest correlation to implanted device size compared to other imaging methods including conventional cardiac angiography and cardiac CT<sup>15-19</sup>. In the current study, we found a 55% agreement rate with the finally implanted device size for TEE. Due to the restricted view by 2D-TEE, underestimation of the LAA ostium diameter can easily

occur if the plane is not exactly aligned with the largest diameter of the LAA orifice<sup>16</sup>. 2D-CT, on the other hand, has been reported rather to overestimate LAA diameters. We show a 77% agreement rate with the final implantation device size, which corresponds closely with the results of Lopez-Minguez et al who reported a 75% agreement rate<sup>18</sup>.

**Table 5. Recommendations of device size by TEE, CT and 3D model compared to finally implanted device size.**

Patient no.	TEE-based recommendation	CT-based recommendation	3D model-based recommendation	Finally implanted device
1	21 ↓	27	27	27
2	24 ↓	30	30	30
3	30	30	30	30
4	30	30	30	30
5	21 ↓	30 ↑	27	27
6	27	27	27	27
7	30	33 ↑	30	30
8	21	21	21	21
9	21	21	21	21
10	21	24 ↑	21	21
11	27	27	27	27
12	24	24	24	24
13	24 ↓	27	27	27
14	24	27 ↑	24	24
15	24	27	27	27
16	30	30	30	30
17	21 ↓	27	27	27
18	30 ↓	33	33	33
19	21 ↓	30	30	30
20	21 ↓	24	24	24
21	24 ↓	33	33	33
22	27 ↓	30 ↓	30 ↓	33

CT: computed tomography; TEE: transoesophageal echocardiography

3D printing technology has been increasingly applied for interventional and surgical procedural planning<sup>6-8</sup>. For optimal LAA device sizing, Otton et al analysed positioning and anatomic deformation of the WATCHMAN device in a flexible 3D printed LAA replica<sup>7</sup>. An implanted 21 mm WATCHMAN in the 3D replica as recommended by TEE sizing showed insufficient radial force and deformation of the LAA, whereas the 27 mm device was too large to achieve full retraction. A 24 mm occluder was deployed showing intraoperative good fitting with no peri-device leak. Pellegrino et al reported two successful cases of LAA occlusion procedures

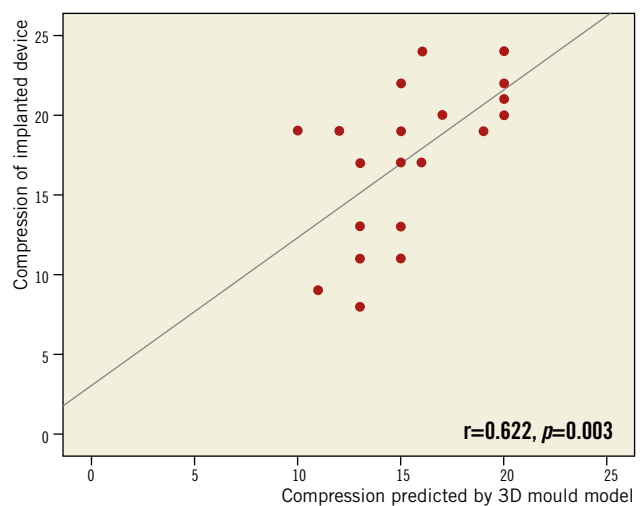


**Figure 5.** Correlation between compression of the finally implanted occluder and compression predicted by the 3D model.

supported by a 3D printed model for device sizing using two different occluder systems (WaveCrest™ [Biosense Webster, Irvine, CA, USA] and AMPLATZER™ Amulet™ [St. Jude Medical, St. Paul, MN, USA])<sup>20</sup>. Liu et al generated LAA printing models from 3D-TEE data and reported a correctly suggested device size in seven out of eight individuals<sup>21</sup>. Wang et al investigated LAA device sizing using a 3D-CT-based approach including 3D printing for planning of spatial navigation through the left atrium<sup>22</sup>. They reported a 100% successful implantation rate for the 3D-CT-predicted sizing, but a slight peri-device leak in 7.5% of the patients. In our study, only optimal implantation results, defined as a completely sealed ostium, a positive tug test and a device compression within optimal range (8-20%), were accepted. Therefore, we counted only 21/22 successful implantations (95%) based on 3D model-based sizing. In the one patient with an undersized occluder, the 3D model-based size prediction resulted in a slightly too small and deeply seated device *in vivo*. As the device size showed a correct position and complete sealing in the 3D model, we assume that the undersizing was most likely due to a reduced LAA filling pressure during CT acquisition despite pre-hydration. The interventionalist therefore decided to perform a full recapture and switch to a 33 mm device. The final result with the implanted 33 mm occluder showed a complete sealing with an optimal compression. In addition to mere sizing, we also assessed the prediction of device compression by the 3D model. An optimal compression of 8-20% has been emphasised to ensure a sufficient pressure on the LAA wall for minimising the risk of embolisation and residual leakages<sup>5</sup>. There was a good correlation between 3D model-predicted compression and compression of the implanted device. Compression of the implanted device was within optimal range in 77% of the cases. Recently, Li et al published a small study on 42 patients randomised to 3D printing-based or conventional imaging-based sizing<sup>23</sup>. They reported no case of residual shunt as assessed by TEE for the 3D print cohort, but 3/21 cases for the conventional imaging cohort. Among procedural parameters, a significant radiation exposure reduction was found.

## Limitations

Several limitations need to be acknowledged. First, our patient cohort included only 22 individuals. Device size selection initially used for implantation was based only on the 3D model, and there was no randomisation to CT-based and TEE-based sizing for device implantation. Therefore, we do not know in how many cases a TEE-sized (and hence probably smaller) device would also have been acceptable for implantation. Next, we created the 3D model based only on CT data, while 3D printing from 3D-TEE data has also been reported, but was not used in this trial. Furthermore, we applied 2D-TEE for preprocedural sizing, which is used for LAA occlusion guidance and device sizing as standard. The superiority of 3D-TEE over 2D-TEE has been demonstrated; however, Wang et al reported an undersizing of 53% for 3D-TEE-based and 62% for 2D-TEE-based size prediction<sup>22,24</sup>. Additionally, patient preparation regarding hydration status is crucial to ensure optimal LAA filling. Prior to CT, TEE and implantation, patients were hydrated, but their hydration status and left atrium

pressure may still have differed slightly. Furthermore, the silicone rubber used for the 3D model does not exactly mimic the specific texture, elasticity and distensibility of the left atrium. Therefore, the silicone models may not fully simulate device compression, since their ability to reshape and expand may be different from LAA tissue. Nonetheless, a 95% correct size prediction and absence of procedure-related complications in our series show that 3D models allow reliable sizing with excellent procedural outcome, supporting the clinical use of 3D printing for LAA occlusion device sizing. Finally, we only addressed the WATCHMAN LAA occluder in the current study. We would expect that the benefit of 3D model sizing should be transferable to alternative occluders, though proof of this assumption must be obtained in specific studies with other occluders.

## Conclusions

We present a proof-of-concept study showing that 3D printing is capable of assisting device selection and prediction of device compression for LAA occlusion using the WATCHMAN device. As a next step, a larger randomised trial consisting of a TEE, CT and 3D model study arm will be needed to assess the outcome of the different sizing approaches.

### Impact on daily practice

Conventional imaging by TEE and CT in the context of LAA occlusion is limited due to the complex three-dimensional and highly variable LAA anatomy. 3D printing has emerged as a potentially useful tool for the planning of structural heart interventions. 3D print models are feasible to assist interventional LAA occlusion for preprocedural device sizing and prediction of device compression.

## Funding

This study was supported by Forschungsstiftung Medizin, Friedrich-Alexander University Erlangen-Nürnberg, and by Manfred-Roth-Stiftung, Fürth.

## Conflict of interest statement

The authors have no conflicts of interest to declare.

## References

1. Kirchhof P, Benussi S, Kotecha D, Ahlsson A, Atar D, Casadei B, Castella M, Diener HC, Heidbuchel H, Hendriks J, Hindricks G, Manolis AS, Oldgren J, Popescu BA, Schotten U, Van Putte B, Vardas P, Agewall S, Camm J, Baron Esquivias G, Budts W, Caceris J, Casselman F, Coca A, De Caterina R, Deffereos S, Dobrev D, Ferro JM, Filippatos G, Fitzsimons D, Gorennek B, Guenoun M, Hohnloser SH, Kolh P, Lip GY, Manolis A, McMurray J, Ponikowski P, Rosenhek R, Ruschitzka F, Savelieva I, Sharma S, Suwalski P, Tamargo JL, Taylor CJ, Van Gelder IC, Voors AA, Windecker S, Zamorano JL, Zeppenfeld K. 2016 ESC Guidelines for the management of atrial fibrillation developed in collaboration with EACTS. *Eur Heart J*. 2016;37:2893-962.

2. Granger CB, Armaganijan LV. Newer oral anticoagulants should be used as first-line agents to prevent thromboembolism in patients with atrial fibrillation and risk factors for stroke or thromboembolism. *Circulation*. 2012;125:159-64.
3. Holmes DR, Reddy VY, Turi ZG, Doshi SK, Sievert H, Buchbinder M, Mullin CM, Sick P; PROTECT AF Investigators. Percutaneous closure of the left atrial appendage versus warfarin therapy for prevention of stroke in patients with atrial fibrillation: a randomised non-inferiority trial. *Lancet*. 2009;374:534-42.
4. Holmes DR Jr, Kar S, Price MJ, Whisenant B, Sievert H, Doshi SK, Huber K, Reddy VY. Prospective randomized evaluation of the Watchman Left Atrial Appendage Closure device in patients with atrial fibrillation versus long-term warfarin therapy: the PREVAIL trial. *J Am Coll Cardiol*. 2014;64:1-12.
5. Meier B, Blaauw Y, Khatib AA, Lewalter T, Sievert H, Tondo C, Glikson M. EHRA/EAPCI expert consensus statement on catheter-based left atrial appendage occlusion. *EuroIntervention*. 2015;10:1109-25.
6. Ripley B, Kelil T, Cheezum MK, Goncalves A, Di Carli MF, Rybicki FJ, Steigner M, Mitsouras D, Blankstein R. 3D printing based on cardiac CT assists anatomic visualization prior to transcatheter aortic valve replacement. *J Cardiovasc Comput Tomogr*. 2016;10:28-36.
7. Otton JM, Spina R, Sulas R, Subbiah RN, Jacobs N, Muller DW, Gunalingam B. Left Atrial Appendage Closure Guided by Personalized 3D-Printed Cardiac Reconstruction. *JACC Cardiovasc Interv*. 2015;8:1004-6.
8. Vukicevic M, Mosadegh B, Min JK, Little SH. Cardiac 3D Printing and its Future Directions. *JACC Cardiovasc Imaging*. 2017;10:171-84.
9. Achenbach S, Goroll T, Seltmann M, Pflederer T, Anders K, Ropers D, Daniel WG, Uder M, Lell M, Marwan M. Detection of coronary artery stenoses by low-dose, prospectively ECG-triggered, high-pitch spiral coronary CT angiography. *JACC Cardiovasc Imaging*. 2011;4:328-37.
10. Wang Y, Di Biase L, Horton RP, Nguyen T, Morhanty P, Natale A. Left atrial appendage studied by computed tomography to help planning for appendage closure device placement. *J Cardiovasc Electrophysiol*. 2010;21:973-82.
11. Romero J, Cao JJ, Garcia MJ, Taub CC. Cardiac imaging for assessment of left atrial appendage stasis and thrombosis. *Nat Rev Cardiol*. 2014;11:470-80.
12. Behnes M, Akin I, Sartorius B, Fastner C, El-Battrawy I, Borggreffe M, Haubenreisser H, Meyer M, Schoenberg SO, Henzler T. --LAA Occluder View for post-implantation Evaluation (LOVE)--standardized imaging proposal evaluating implanted left atrial appendage occlusion devices by cardiac computed tomography. *BMC Med Imaging*. 2016;16:25.
13. Israel CW, Tschishow WN, Ridjab D, Kische S, Buddecke J, Ince H. [Implantation of Watchman™ occluder of the left atrial appendage. Tips and tricks]. [Article in German]. *Herzschrittmacherther Elektrophysiol*. 2013;24:39-52.
14. Boersma LV, Schmidt B, Betts TR, Sievert H, Tamburino C, Teiger E, Pokushalov E, Kische S, Schmitz T, Stein KM, Bergmann MW; EWOLUTION investigators. Implant success and safety of left atrial appendage closure with the WATCHMAN device: peri-procedural outcomes from the EWOLUTION registry. *Eur Heart J*. 2016;37:2465-74.
15. Krishnaswamy A, Patel NS, Ozkan A, Agarwal S, Griffin BP, Saliba W, Tuzcu EM, Schoenhagen P, Kapadia SR. Planning left atrial appendage occlusion using cardiac multidetector computed tomography. *Int J Cardiol*. 2012;158:313-7.
16. Clemente A, Avoglierio F, Berti S, Paradossi U, Jamagidze G, Rezzaghi M, Della Latta D, Chiappino D. Multimodality imaging in preoperative assessment of left atrial appendage transcatheter occlusion with the Amplatzer Cardiac Plug. *Eur Heart J Cardiovasc Imaging*. 2015;16:1276-87.
17. Sievert H, Lesh MD, Trepels T, Omran H, Bartorelli A, Della Bella P, Nakai T, Reisman M, DiMario C, Block P, Kramer P, Fleschenberg D, Krumsdorf U, Scherer D. Percutaneous left atrial appendage transcatheter occlusion to prevent stroke in high-risk patients with atrial fibrillation: early clinical experience. *Circulation*. 2002;105:1887-9.
18. Lopez-Minguez JR, Gonzalez-Fernandez R, Fernandez-Vegas C, Millan-Nunez V, Fuentes-Canamero ME, Nogales-Asensio JM, Doncel-Vecino J, Elduayen-Gragera J, Ho SY, Sanchez-Quintana D. Anatomical classification of left atrial appendages in specimens applicable to CT imaging techniques for implantation of amplatzer cardiac plug. *J Cardiovasc Electrophysiol*. 2014;25:976-84.
19. Budge LP, Shaffer KM, Moorman JR, Lake DE, Ferguson JD, Mangrum JM. Analysis of in vivo left atrial appendage morphology in patients with atrial fibrillation: a direct comparison of transesophageal echocardiography, planar cardiac CT, and segmented three-dimensional cardiac CT. *J Interv Card Electrophysiol*. 2008;23:87-93.
20. Pellegrino PL, Fassini G, Di Biase M, Tondo C. Left Atrial Appendage Closure Guided by 3D Printed Cardiac Reconstruction: Emerging Directions and Future Trends. *J Cardiovasc Electrophysiol*. 2016;27:768-71.
21. Liu P, Liu R, Zhang Y, Liu Y, Tang X, Cheng Y. The Value of 3D Printing Models of Left Atrial Appendage Using Real-Time 3D Transesophageal Echocardiographic Data in Left Atrial Appendage Occlusion: Applications toward an Era of Truly Personalized Medicine. *Cardiology*. 2016;135:255-61.
22. Wang DD, Eng M, Kupsky D, Myers E, Forbes M, Rahman M, Zaidan M, Parikh S, Wyman J, Pantelic M, Song T, Nadig J, Karabon P, Greenbaum A, O'Neill W. Application of 3-Dimensional Computed Tomographic Image Guidance to WATCHMAN Implantation and Impact on Early Operator Learning Curve: Single-Center Experience. *JACC Cardiovasc Interv*. 2016;9:2329-40.
23. Li H, Qingyao, Bingshen, Shu M, Lizhong, Wang X, Song Z. Application of 3D printing technology to left atrial appendage occlusion. *Int J Cardiol*. 2017;231:258-63.
24. Goebel B, Wieg S, Hamadanchi A, Otto S, Jung C, Kretzschmar D, Figulla HR, Christian Schulze P, Poerner TC. Interventional left atrial appendage occlusion: added value of 3D transesophageal echocardiography for device sizing. *Int J Cardiovasc Imaging*. 2016;32:1363-70.